Available online at www.sciencedirect.com
SCIENCE DIRECT
Catalysis Today 101 (2005) 15–21
CATALYSIS TODAY
www.elsevier.com/locate/cattod

Influence of the addition of promoters to steam reforming catalysts

Juliana da S. Lisboa [a], Danielle C.R.M. Santos [a], Fabio B. Passos [a,*], Fabio B. Noronha [b,1]

[a] *Departamento de Engenharia Química, Universidade Federal Fluminense (UFF), Rua Passo da Pátria, 156-CEP 24210-240 Niterói, RJ, Brasil*
[b] *Instituto Nacional de Tecnologia (INT), Laboratório de Catálise, Av. Venezuela, 82-CEP, 20084-310 Rio de Janeiro, RJ, Brasil*

Abstract

The steam reforming of hydrocarbons may be catalyzed by several transition metals. The most frequently used catalysts are α-Al_2O_3 supported nickel-based catalysts, which are frequently modified by the addition of promoters such as Mg and Ca, in order to improve their stability and selectivity. The mechanism of promotion was investigated using temperature programmed surface reaction (TPSR), diffuse reflectance UV–vis spectroscopy (DRS) and temperature-programmed oxidation. The DRS spectra showed bands characteristic to NiO with Al^{3+} and NiO with less interaction with the support. Temperature programmed surface reaction results showed that there is an increase in the reforming activity by the presence of the promoters, without modification in the mechanism of reaction. The TPO results showed that the addition of promoters caused an increase on the hydrogen content of the coke formed.

Keywords: Steam reforming; Promoters; Ni; Synthesis gas

1. Introduction

Synthesis gas is a fundamental feedstock for refining processes, such as hydrotreating and hydrocracking, and for petrochemical processes, such as the synthesis of methanol, methanol to gasoline, and the synthesis of ammonia [1,2]. Synthesis gas is also a key feedstock for the hydrocarbon synthesis via Fischer–Tropsch processes [3,4]. Natural gas and other hydrocarbons are the dominant feedstock for the production of synthesis gas because the investments are about one-third of a coal based plant [5]. Furthermore, environmental restrictions in the fuel market are opening a window of opportunity for marketing synthetic fuels from natural gas (GTL technology). Several governments are imposing restrictions on gas flaring and ventilation, which represents emissions of greenhouse gases and non-burned hydrocarbons, contributing for global warming and ozone depletion. Moreover, synthetic fuels are sulfur-free and have a high performance fulfilling the new patterns for fuel quality and level of pollutants [5].

Synthesis gas manufacture stands for about 60% of the investment of large-scale GTL plants [6]. In this way, the optimization of synthesis gas manufacture is beneficial for the economic viability of GTL plants. Steam reforming is the main industrial process to produce synthesis gas, but it produces a H_2/CO ratio close to 3. The Fischer–Tropsch synthesis requires a H_2/CO ratio close to 2 [3], which may be obtained by combining the steam reforming with partial oxidation in the so called autothermal reforming [5]. In this process, the required H_2/CO ratio is obtained using low steam-to-carbon ratios and high exit temperatures [5]. Under these reaction conditions, deactivation of the catalyst due to carbon deposition on its surface occurs.

Commercial catalysts for steam reforming are usually supported Ni catalysts. Earth alkaline metals (Mg and Ca) are frequently used in the catalyst formulations to improve stability [7], and their effect was attributed to the increase of the steam–carbon reaction and to the neutralization of the acidity of the support, suppressing cracking and polymerization reactions [7]. The suppression of carbon deposition was also explained by nickel ensemble control [5]. In the current work, we further investigated the effect of the addition of Mg and Ca to steam reforming catalysts using UV–vis diffuse reflectance spectroscopy (DRS), temperature programmed surface reaction (TPSR) and temperature

* Corresponding author. Tel.: +55 21 2629 5600; fax: +55 21 2722 2069.
E-mail addresses: fbpassos@engenharia.uff.br (F.B. Passos), fabiobel@int.gov.br (F.B. Noronha).
[1] Tel.: +55 21 2206 1163; fax: +55 21 2206 1164.

0920-5861/$ – see front matter © 2005 Elsevier B.V. All rights reserved.
doi:10.1016/j.cattod.2004.12.005

programmed oxidation (TPO) besides probing the surface with cyclohexane conversion.

2. Experimental

2.1. Catalyst preparation

The support used was α-Al_2O_3 (ALCOA 1.5 m^2/g). Ni/α-Al_2O_3 catalysts with 5, 10 and 20 wt.% were prepared by incipient wetness impregnation, using $Ni(NO_3)_2{\cdot}6H_2O$ as precursor. After impregnation, the samples were dried at 120 °C and calcined at 650 °C for 6 h. A 20 wt.% Ni/α-Al_2O_3 sample was also prepared by wet impregnation. The drying and calcination procedures were the same as those used for the samples prepared by incipient wetness.

Mg- and Ca-containing catalysts were prepared by incipient wetness impregnation of α-Al_2O_3 with $Mg(NO_3)_2{\cdot}6H_2O$ or $Ca(NO_3)_2{\cdot}4H_2O$ precursors, followed by drying at 120 °C and calcination at 650 °C [8]. The samples were then impregnated with the $Ni(NO_3)_2{\cdot}6H_2O$ aqueous solution, followed by the drying and calcination procedures already cited. By this procedure, 5 wt.% MgO–10 wt.% Ni/α-Al_2O_3, 5 wt.% CaO–10 wt.% Ni/α-Al_2O_3 and 5 wt.% MgO–5 wt.%CaO–10 wt.% Ni/α-Al_2O_3 catalysts were obtained.

2.2. UV–vis diffuse reflectance spectroscopy

The samples were characterized at room temperature in a VARIAN-Cary 500 UV–vis spectrophotometer equipped with a diffuse reflectance accessory (Harrick). In order to separate the contribution of the support, the reflectance $R(\lambda)$ of the sample was made proportional to the reflectance of α-Al_2O_3, and the Kubelka–Munk function $F(R)$ was calculated.

2.3. Temperature programmed surface reaction

TPSR experiments were performed in a multipurpose unit coupled to a Balzers Omnistar quadrupole mass spectrometer. The samples (27 mg) were previously dried at 150 °C for 30 min under He flow (30 mL/min), followed by reduction under H_2 flow at 800 °C, for 2 h and cooled in He to room temperature. The sample was then submitted to a reactant mixture containing pure H_2, CH_4, He and H_2O in a volumetric ratio of 32:27:33:8, at a flow rate of 200 mL/min and the temperature was raised to 800 °C at a heating rate of 20 °C/min. The feed composition was similar to one used in reference [9].

2.4. Temperature programmed oxidation

TPO experiments were performed in the same multipurpose unit used for the previous technique. The samples (200 mg) were previously dried at 150 °C for 30 min, under He flow (30 mL/min), followed by reduction under H_2 at 800 °C, for 2 h, and treatment under CH_4 flow for 60 min at 800 °C. The samples were cooled to room temperature, followed by an increase of temperature under O_2/He (30 mL/min) flow in a rate of 10 °C/min to 800 °C.

2.5. H_2 and CO chemisorption

H_2 and CO chemisorption uptakes were measured by using pulses of a mixture containing 5%H_2 in Ar and 10%CO in He, respectively, at room temperature. This experiment was performed on the same apparatus described to the TPR measurements and the samples were submitted to the same pretreatment used in TPSR experiments.

2.6. Cyclohexane conversion

Cyclohexane conversion was performed at 10^5 Pa in a flow microreactor. The samples (100 mg) were previously dried at 150 °C for 30 min under N_2 flow (30 mL/min) and reduced at 500 °C under H_2 flow (30 mL/min). The reactant mixture was obtained by bubbling hydrogen through a saturator containing cyclohexane at 12 °C (H_2/C_6H_{12} = 13.6). The temperature was kept at 320 °C and the conversion was kept below 10%. The effluent gas phase was analyzed by an on-line gas chromatograph (HP 5890) equipped with a flame ionization detector and an HP-Innowax capillary column. Under these conditions, there was no significant deactivation of the catalysts and there were no diffusional or thermodynamic limitations.

3. Results

3.1. UV–vis diffuse reflectance spectroscopy

DRS profiles for the catalysts with and without promoters are shown in Figs. 1 and 2. The presence of nickel aluminate

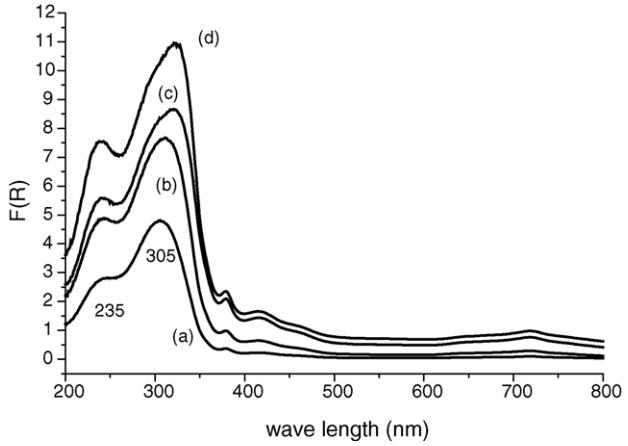

Fig. 1. UV–vis DRS profiles of catalysts: (a) 5% Ni/α-Al_2O_3; (b) 10% Ni/α-Al_2O_3; (c) 20% Ni/α-Al_2O_3 (wet impregnation); (d) 20% Ni/α-Al_2O_3.

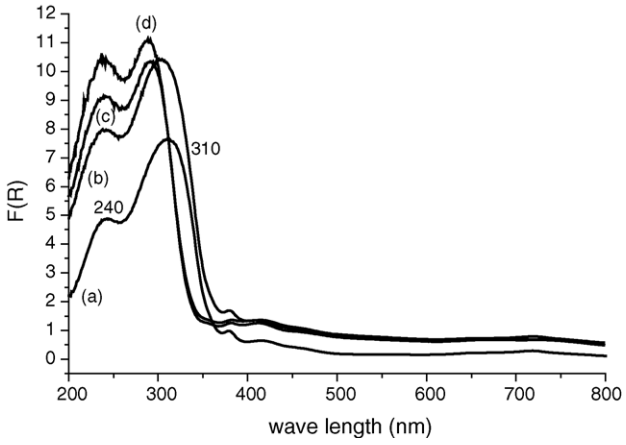

Fig. 2. UV–vis DRS profiles of catalysts: (a) 10% Ni/α-Al_2O_3; (b) 5% MgO–10% Ni/α-Al_2O_3; (c) 5%CaO–10% Ni/α-Al_2O_3; (d) 5% MgO–5%CaO–10% Ni/α-Al_2O_3.

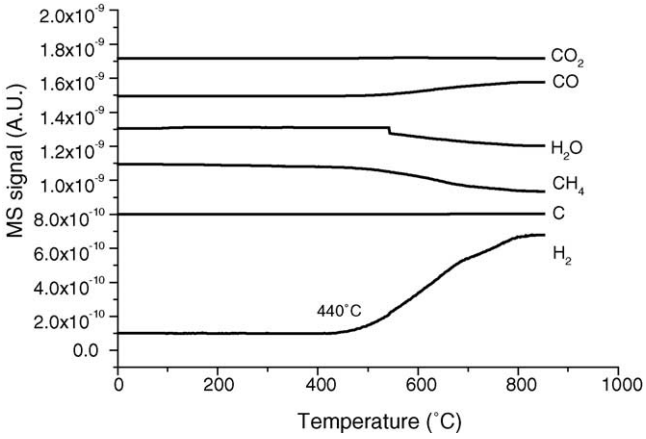

Fig. 3. TPSR profiles for 5% Ni/α-Al_2O_3 catalyst.

was not detected in any of the prepared catalysts, due to the calcination temperature of the samples. Two bands around 235 and 305 nm were observed for all the samples. Bands in this range for Ni catalyst are usually ascribed to charge transfer of octahedral Ni^{2+} species [10]. From previous temperature-programmed reduction studies [11,12], we may explain the occurrence of these two bands: the first by the formation of NiO with Al^{3+} ions incorporated due to the dissolution of α-Al_2O_3 during the impregnation step, and the second to NiO with less interaction with the support, for catalysts with and without promoters.

3.2. H_2 and CO chemisorption

H_2 and CO chemisorption uptakes are shown in Table 1. Dispersions were not calculated as reduction degrees of Ni catalysts are not known. The H_2 and CO uptakes were relatively low, as typically observed for high content Ni catalysts. These low values were also due to the low surface area of the used support (1.5 m^2/g) and to the high calcination and reduction temperatures employed. This way, it is quite difficult to obtain trends from these results, but the addition of Mg seemed to increase H_2 and CO uptakes.

Table 1
CO and H_2 chemisorption uptakes on Ni catalysts after reduction at 800 °C

Catalyst	H_2 irreversible chemisorption ($\mu mol/g_{cat}$)	CO irreversible chemisorption ($\mu mol/g_{cat}$)
5% Ni/α-Al_2O_3	3.9	7.8
10% Ni/α-Al_2O_3	4.6	7.9
20% Ni/α-Al_2O_3	2.2	7.2
20% Ni/α-Al_2O_3 (wet impregnation)	1.3	4.7
5% MgO–10% Ni/α-Al_2O_3	8.2	19.3
5% CaO–10% Ni/α-Al_2O_3	2.8	4.1
5% MgO–5% CaO–10% Ni/α-Al_2O_3	10.4	15.2

3.3. Temperature programmed surface reaction

The profiles of temperature programmed surface reaction for the 5% Ni/α-Al_2O_3 catalyst and for the 5%CaO/10%Ni/α-Al_2O_3 are shown in Figs. 3 and 4, respectively, and are representative of all catalysts. Similar reaction profiles were observed in all cases, with initial reaction temperature varying from 440 °C (for 5% Ni/α-Al_2O_3 catalyst) to 470 °C (for 5%CaO/10%Ni/α-Al_2O_3 catalyst). CO_2 formation was not observed. Table 2 shows methane conversion estimated at the end of TPSR experiments, obtained from the mass spectrometer signals. The conversion of CH_4 was close to 10% for catalysts containing only nickel, independently of nickel content present in the samples. For catalysts containing Ca and/or Mg, there was an increase in CH_4 conversion leading to values to around 20%.

3.4. Temperature programmed oxidation

The CO_2 formation profiles obtained in the temperature programmed oxidation experiments for the catalysts with

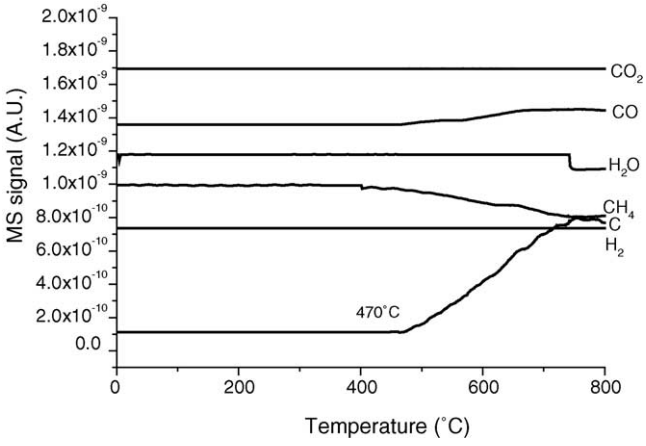

Fig. 4. TPSR profiles for 5%CaO/10% Ni/α-Al_2O_3 catalyst.

Table 2
CH_4 conversion at the end of TPSR experiments

Catalysts	CH_4 conversion (%)
5% Ni/α-Al_2O_3	13
10% Ni/α-Al_2O_3	8
20% Ni/α-Al_2O_3	13
20% Ni/α-Al_2O_3 (wet impregnation)	10
5%MgO–10% Ni/α-Al_2O_3	19
5%CaO–10% Ni/α-Al_2O_3	19
5%MgO–5%CaO–10% Ni/α-Al_2O_3	21

and without promoters are shown in Figs. 5 and 6, as follows. The carbon oxidation began next to 500 °C for all catalysts, and the highest temperature was between 600 and 650 °C, varying with Ni content. The presence of water was not identified for 5 and 10% Ni catalysts, confirming the formation of unique type of coke. For the other catalysts, a small amount of water was formed during the oxidation experiment. On unpromoted Ni/Al_2O_3 catalysts, there was the occurrence of a peak and a shoulder showing the existence of two types of carbon deposited on catalysts surface. For the promoted catalysts there was an increase in the lower temperature peak (around 550 °C). Table 3 shows the total quantities of CO_2 formed for the several catalysts. The CO_2 formation increased with the addition of promoters and as the Ni content increased.

A second temperature programmed oxidation experiment was performed after the temperature programmed surface reaction. Fig. 7 shows that the catalysts with 5 and 10 wt.% nickel contents presented only one type of carbon formed, being consistent with the same tendency observed in the TPO experiment performed without TPSR occurrence. Besides, Fig. 8 showed Mg addition lead to the formation of a second type of coke with a higher content of H_2, and that was more easily oxidized.

Table 4 shows the total quantities of CO_2 formed during the TPO experiments performed after the TPSR experiments, and it can be noticed that the addition of promoters increased the amount of coke formed in the conditions investigated.

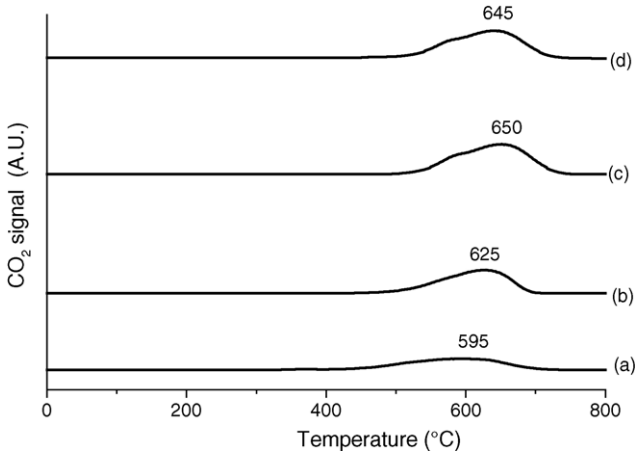

Fig. 5. TPO profiles obtained for the catalysts: (a) 5% Ni/α-Al_2O_3; (b) 10% Ni/α-Al_2O_3; (c) 20% Ni/α-Al_2O_3; (d) 20% Ni/α-Al_2O_3 (wet impregnation).

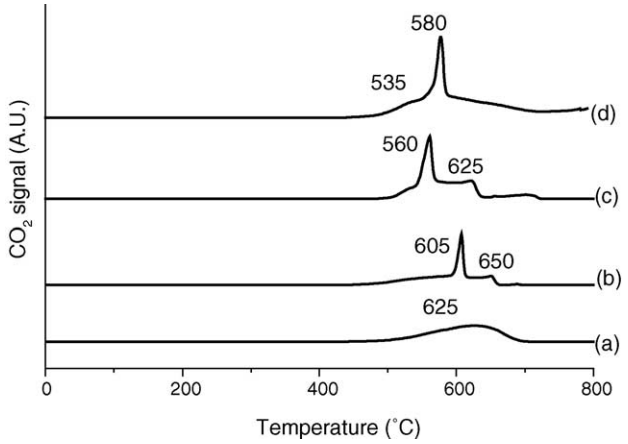

Fig. 6. TPO profiles obtained for the catalysts: (a) 10% Ni/α-Al_2O_3; (b) 5% MgO–10% Ni/α-Al_2O_3; (c) 5%CaO–10% Ni/α-Al_2O_3; (d) 5% MgO–5%CaO–10% Ni/α-Al_2O_3.

3.5. Cyclohexane conversion

Table 5 displays the results obtained for the several catalysts in the cyclohexane conversion. Turnover frequencies (TOF) were calculated using CO chemisorption uptakes obtained in the very same conditions as the pretreatment of the samples for the reaction. The conversion of cyclohexane proceeded through two reaction pathways, dehydrogenation and hydrogenolysis. Essentially, the turnover frequency for the dehydrogenation reaction was not modified by the addition of the promoters. However, the hydrogenolysis was suppressed when Mg was present in the catalyst, indicating a modification of Ni particles.

4. Discussion

The obtained results indicate modification of Ni particles by the presence of Mg. This modification takes place probably during the reduction step, as the DRS-UV–vis

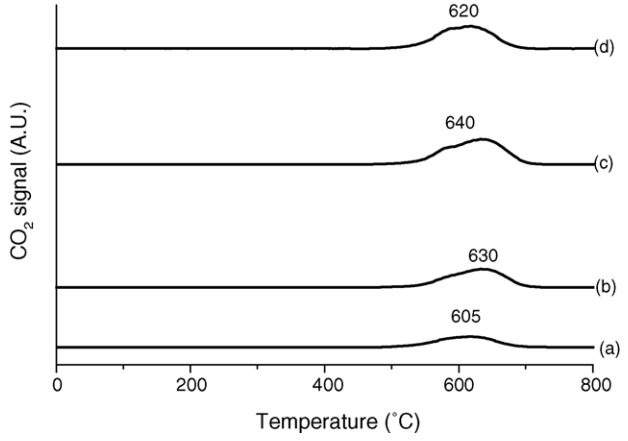

Fig. 7. TPO profiles obtained for the catalysts after TPSR experiments: (a) 5% Ni/α-Al_2O_3; (b) 10% Ni/α-Al_2O_3; (c) 20% Ni/α-Al_2O_3; (d) 20% Ni/α-Al_2O_3 (wet impregnation).

Table 3
Amount of CO_2 formed during TPO of coked Ni catalyst

Catalysts	Amount of CO_2 formed (mmol/g_{cat})
5% Ni/α-Al_2O_3	0.35
10% Ni/α-Al_2O_3	0.56
20% Ni/α-Al_2O_3	0.82
20% Ni/α-Al_2O_3 (wet impregnation)	0.77
5%MgO–10% Ni/α-Al_2O_3	1.5
5%CaO–10% Ni/α-Al_2O_3	1.3
5%MgO–5%CaO–10% Ni/α-Al_2O_3	1.7

spectra of the several precursors, after calcinations, showed similar results for promoted and non-promoted samples.

TPSR experiments showed only methane steam reforming occurred in the conditions tested, and this was not influenced by the presence of promoters. Wei and Iglesia [13] reported recently that the rate-determining step for methane conversions is the C–H bond activation, with the kinetics following a first-order power-law model. Thus, the increase in the conversion of methane observed during the TPSR experiments is related to a higher amount of active sites available for the reaction. This could be caused by an increase in the exposed metal surface area and also by an inhibition of metal surface blocking by coke deposits. This way, for the non-promoted catalysts, chemisorption results showed similar metal surface areas leading to similar final conversions in the TPSR experiments. The chemisorption results also indicated an increase in exposed metal area by the addition of the promoters, however an effect on coke formation could also be observed by the TPO experiments, with the amount of coke observed being higher for the promoted catalysts. Fig. 9 shows that coke formation during the TPSR experiments correlates fairly well with the conversion. The higher conversion of methane caused a higher formation of coke, but in the presence of the promoters the formed coke did not block the nickel surface for the reaction.

Coke formation is inherent to the steam reforming reaction. According to the literature [14], the methane decomposition can produce three types of surface carbonaceous species. Methane dissociates on the nickel surface to generate highly reactive carbon species (C_α) [15]. The carbidic carbon can be gasified or converted to a less active

Table 4
Amount of CO_2 formed during TPO performed after TPSR for Ni catalysts

Catalysts	CO_2 formed (mmol/g cat)
5% Ni/α-Al_2O_3	1.7
10% Ni/α-Al_2O_3	2.7
20% Ni/α-Al_2O_3	4.7
20% Ni/α-Al_2O_3 (wet impregnation)	5.4
5%MgO–10% Ni/α-Al_2O_3	9.1
5%CaO–10% Ni/α-Al_2O_3	8.8
5%MgO–5%CaO–10% Ni/α-Al_2O_3	11.6

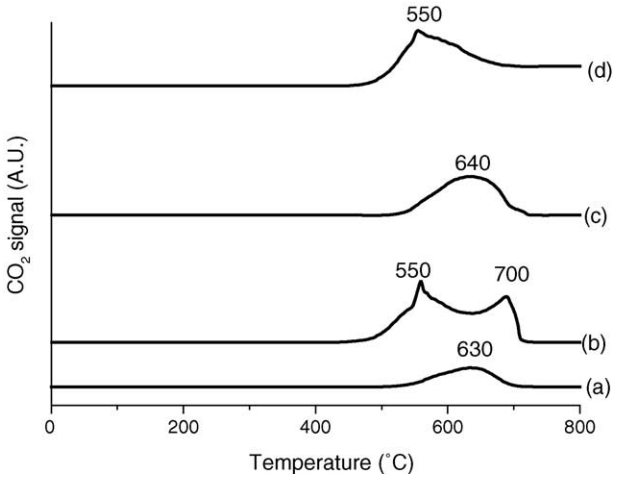

Fig. 8. TPO profiles obtained for the catalysts after TPSR: (a) 10% Ni/α-Al_2O_3; (b) 5% MgO–10% Ni/α-Al_2O_3; (c) 5%CaO–10% Ni/α-Al_2O_3; (d) 5% MgO–5%CaO–10% Ni/α-Al_2O_3.

C_β (amorphous carbon) by polymerization. C_β may be gasified or may dissolve in the nickel crystallite, which leads to the formation of a carbon whisker. A third type of carbon species comprises the graphitic carbon (C_γ). These carbon species show different reactivity towards oxidation and hydrogenation. For example, carbidic carbon is hydrogenated at temperatures below 323 K whereas graphitic carbon is hydrogenable at temperatures higher than 673 K. TPO experiments of carbonaceous species formed on Ni/CaO–Al_2O_3 exhibited two peaks at low (873 K) and high (1000 K) temperatures [16]. The high temperature peak was assigned to amorphous and/or graphite forms of carbon. The low temperature peak of CO_2 was attributed to filamentous carbon associated with dissolution of carbon into the bulk of nickel crystallites. Zhang and Verykios [17] showed that the stability of a 17 wt.% Ni/Al_2O_3 catalyst was improved by the addition of CaO in the support. TPO analyses revealed that

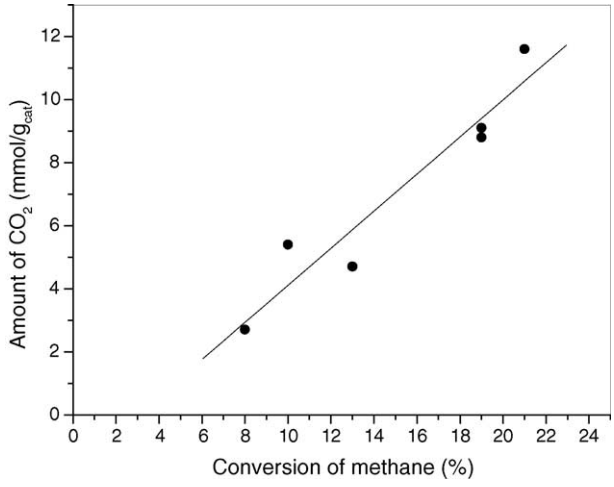

Fig. 9. Correlation between the final conversion of methane in TPSR experiments and the amount of CO_2 formed during TPO experiments performed after the TPSR for Ni catalysts.

Table 5
CO chemisorption uptakes and TOF for cyclohexane conversion on supported Ni catalysts (T = 373 K; H_2/CH = 13.2)

Catalyst	CO irreversible chemisorption ($\mu mol/g_{cat}$)	TOF for dehydrogenation (s^{-1})	TOF for hydrogenolysis (s^{-1})
5% Ni/α-Al_2O_3	8.4	0.53	0.11
10% Ni/α-Al_2O_3	11.6	0.36	0.18
20% Ni/α-Al_2O_3	22.8	0.17	0.11
20% Ni/α-Al_2O_3 (wet impregnation)	19.1	0.16	0.13
5% MgO–10% Ni/α-Al_2O_3	4.6	0.43	0
5% CaO–10% Ni/α-Al_2O_3	14.7	0.17	0.15
5% MgO–5% CaO–10% Ni/α-Al_2O_3	6.4	0.14	0

the improved stability of promoted catalyst was probably due to the enhanced reactivity of carbon formed under reforming reaction conditions.

Therefore, the TPO peak at low temperature could be attributed to the oxidation of a more reactive carbon species (C_α). The CO_2 formation at high temperature may be ascribed to well crystalline graphite carbon. Similar TPO peak assignments were reported by Swaan et al. [18] and by Wang and Lu [19]. These results suggest that the addition of promoters reduces the formation of a less reactive carbon and hence improves the resistance to the carbon formation, although the total amount of coke may be higher. Lodeng et al. [20] showed that the addition of promoters increases the initial coke formation rate, but for long deactivation periods, the total quantity of coke formed is smaller for promoted catalysts than for catalysts without promoters. In our case, coking time was relatively short (60 min), what explains this increase in coke formation in the presence of promoters.

This promotional effect of Mg can be understood through the size of nickel ensembles. The size of the ensemble is closely related to carbon formation on the steam reforming [5]. The formation of the whisker carbon precursor, C_β, through polymerization/isomerization of C_α requires twice the number of sites necessary to dissociate methane to form C_α [15]. DFT studies showed that adsorbed atomic carbon is more stable at steps than at terraces, with a graphene island growing from the step [21]. There is a critical island size above which the graphene is more stable than carbon atoms adsorbed along the step, implying that the smaller the ensemble size the more difficult is the deactivation by coke formation [5]. Our cyclohexane conversion experiments gave results very consistent to this hypothesis. The turnover frequency for dehydrogenation route was not influenced by the addition of the promoters, what is in agreement to the structure-insensitivity of this pathway [22]. However, the hydrogenolysis reaction was suppressed by the addition of Mg. As the hydrogenolysis is a structure-sensitive reaction [23], this result indicates that the presence of Mg reduces the Ni ensemble particle size, probably by decoration of Ni particles by Mg. This may explain the beneficial effect of Mg to steam reforming catalysts, inhibiting the formation of less reactive coke by bloking the steps necessary to nucleation of graphene. In the case of Ca addition, however, we have not observed a modification of Ni particles, and its promotion properties are probably explained by its property to enhance gasification of adsorbed carbon.

5. Conclusions

The results showed that the presence of Ca and Mg favors the steam methane reforming reaction, without changing the reaction mechanism as shown by TPSR experiments. In these catalysts, Ni is present as NiO with incorporation of Al^{3+} ions originating from the dissolution of α-Al_2O_3 during the impregnation step and as NiO with less interaction with the support

The Mg addition caused the formation of coke more easily oxidized and with higher hydrogen content, being able to explain the beneficial effect of this promoter. The temperature programmed oxidation profiles for catalysts without promoters showed the formation of only one type of coke in catalysts with 5 and 10% Ni contents and two types of coke in the other catalysts. In the presence of promoters, a small amount of water was formed with two types of carbon deposited on catalyst surfaces. Conversion of cyclohexane results demonstrated there is an ensemble effect with Mg atoms dilution Ni particles what may explain the beneficial effect of this promoter.

Acknowledgments

The authors are grateful for the financial support received from FAPERJ, PADCT-III and CNPq/CTPetro.

References

[1] M.A. Peña, J.P. Gómez, J.L.G. Fierro, Appl. Catal. A: Gen. 7 (1996) 144.
[2] J.R. Rostrup-Nielsen, in: J.R. Anderson, M. Boudart (Eds.), Catalysis: Science and Technology, vol. 5, Springer-Verlag, New York, 1984, p. 1.
[3] R.B. Anderson, The Fischer-Tropsch Synthesis, Academic Press, New York, 1984.
[4] M.E. Dry, in: J.R. Anderson, M. Boudart (Eds.), Catalysis: Science and Technology, vol. 1, Springer-Verlag, New York, 1984, p. 106.
[5] J.R. Rostrup-Nielsen, J. Sehested, J.K. Nørskov, Adv. Catal. 47 (2002) 65.
[6] K. Aasberg-Petersen, T.S. Christensen, C.S. Nielsen, I. Dybkjaer, Fuel Process Tech. 83 (2003) 253.
[7] M.V. Twigg, Catalyst Handbook, 2nd ed. Manson Publishing, London, 1997.
[8] Z. Cheng, Q. Wu, Z. Yoshuda, Catal. Today 30 (1996) 147.
[9] I. Ul-Haque, D.L. Trimm, E.P. Patent 470626, 1992.

[10] E. Kis, R. Marinkovíc-Neducin, G. Lomic, G. Boskovic, D.Z. Obadovic, J. Kiurski, P. Putanov, Polyhedron 17 (1998) 27.
[11] D.C.R.M. Santos, J.S. Lisboa, F.B. Passos, F.B. Noronha, Braz. J. Chem. Eng 21 (2004) 203.
[12] J.T. Richardson, M.V. Twigg, Appl. Catal. A: Gen. 167 (1998) 57.
[13] J. Wei, E. Iglesia, J. Catal. 224 (204) (2004).
[14] C.H. Bartholomew, Chem. Eng. 91 (1984) 96.
[15] D.L. Trimm, Catal. Today 37 (1997) 233.
[16] M.A. Goula, A.A. Lemonidou, A.M. Efstathiou, J. Catal. 161 (1996) 626.
[17] Z.L. Zhang, X.E. Verykios, Catal. Today 21 (1994) 589.
[18] H.M. Swaan, V.C.H. Kroll, G.A. Martin, C. Mirodatos, Catal. Today 21 (1994) 571.
[19] S. Wang, G.Q.M. Lu, Appl. Catal. B: Environ. 16 (1998) 269.
[20] R. Lodeng, M. Barré-Chassonery, M. Fathi, O.A. Rokstad, A. Holmen, Stud. Surf. Sci. Catal. 111 (1997) 561.
[21] H.S. Bengaard, J.K. Nørskov, J.S. Sehested, B.S. Clausen, L.P. Nielsen, A.M. Molenbrock, J.R. Rostrup-Nielsen, J. Catal. 209 (2002) 365.
[22] F.B. Passos, R. Fréty, M. Schmal, Catal. Lett. 29 (1994) 109.
[23] J.H. Sinfelt, Bimetallic Catalysts: Discoveries, Concepts and Applications, Wiley, New York, 1983.